Size Scaling of Turbulent Transport in Tokamak Plasmas

Z. Lin*, T. S. Hahm, S. Ethier, W. W. Lee, J. Lewandowski,
G. Rewoldt, W. M. Tang, W. X. Wang, L. Chen*, and P. H. Diamond†

Princeton Plasma Physics Laboratory, Princeton, NJ 08543, USA

*Department of Physics and Astronomy,
University of California, Irvine, CA 92697, USA

†Department of Physics,
University of California at San Diego, CA 92093, USA

E-mail: zlin@pppl.gov

October 4, 2002

Abstract

This paper reports that: (1) global gyrokinetic particle simulations of electrostatic ion temperature gradient turbulence show that the fluctuation scale length is microscopic and independent of device size, while the transport coefficient exhibits a gradual transition from a Bohm-like scaling for device sizes corresponding to present-day tokamak experiments to a gyro-Bohm scaling for future larger devices; (2) a nonlinear model for turbulence radial spreading based on the modified porous-medium equation offers a phenomenological understanding of the transition from Bohm to gyro-Bohm scaling; (3) quantitative agreement is obtained between global and local simulations in the gyro-Bohm regime; and (4) we estimate the role of the trapped electron nonlinearity in zonal flow generation in trapped electron mode turbulence in the context of parametric instability theory.

1 Introduction

An accurate prediction of the expected transport level is critical for the design of fusion reactors since the balance between turbulent transport and heating power determines the performance of magnetic fusion plasmas. At present, the reactor design studies [1] rely on extrapolations of turbulent transport properties from present-day tokamak experiments to larger devices. These estimates are based in large part on some forms of empirical scaling, particularly device size scaling, for the global energy confinement time. These empirical scaling estimates are not always compatible with theoretical constraints from transformation invariants of fundamental plasma equations [2]. In this work, transport scaling with respect to device size is critically examined using first-principles gyrokinetic particle simulations for electrostatic toroidal ion

temperature gradient (ITG) turbulence [3], which is a leading candidate to account for anomalous ion thermal transport in the tokamak core region. These large scale nonlinear simulations have recently been enabled by advances in efficient algorithms and by effective utilization of tera-scale massively parallel computers. Our simulation results show that extrapolations based on empirical scalings or mixing length rules can be unreliable and that full device nonlinear simulations can play a key role in complementing and then eventually replacing extrapolation methods by directly addressing parameter regimes inaccessible through conventional analytic or experimental approaches.

In the absence of a fundamental, first-principles turbulence theory, heuristic, mixing length rules are often utilized to estimate size scaling of turbulent transport [3]. This approach invokes a random walk type of picture for diffusive processes using the scale length of turbulent eddies as the step size and the linear growth time of the instability as the step time. It predicts that if the eddy size increases with device size, the transport scaling is Bohm-like, i.e., local ion heat diffusivity is proportional to $\chi_B = cT/eB$. Here c, T, e, B are, respectively, speed of light, electron temperature, electric charge of electrons, and magnetic field amplitude. On the other hand, if the eddy size is microscopic (on the order of the ion gyroradius), the transport scaling is gyro-Bohm, i.e., local ion heat diffusivity is proportional to $\chi_{\rm GB} = \rho^* \chi_B$. Here, $\rho^* = \rho_i/a$ is the ion gyroradius ρ_i normalized by the tokamak minor radius a. If transport is not diffusive (e.g., large transport events dominate the contribution to energy fluxes) the scaling can also be Bohm-like. Most theories [3] and local (or flux-tube) direct simulations [4] of ITG turbulence predict a gyro-Bohm scaling for ion transport since they assume fluctuations on a microscopic scale length and ignore pressure gradient profile variations. The gyroBohm scaling is often the implied scaling in reactor designs [1], and is clearly beneficial for larger devices since it predicts that transport coefficient decreases when the device size increases. However, trends from experimental observations have been more complicated. Transport scalings in low confinement regimes (L-mode) have always been observed to be Bohm or worse than Bohm in major tokamaks [5, 6]. In particular, dimensionless scaling studies on the DIII-D tokamak found that ion transport and energy confinement time exhibit Bohm-like behavior, while fluctuation characteristics suggest a gyro-Bohm scaling [7] for transport. In the high confinement regime (H-mode), transport scalings have been reported to be either Bohm [8] or gyroBohm in limited operational parameter space [6]. The uncertainty reflects the difficulty in varying ρ^* while keeping all other dimensionless parameters fixed (e.g., toroidal Mach number in H-mode).

An effective tool for scaling studies is full torus gyrokinetic particle simulations [9]. In these large scale calculations, kinetic effects and global profile variations are treated rigorously, and ρ^* can be varied for a wide range while all other dimensionless parameters are fixed. In previous global gyrokinetic simulations of electrostatic ITG turbulence, Bohm-like transport scaling was observed due to radially elongated eddies associated with the global structure of linear toroidal eigenmodes [10]. However, those scaling studies did not properly deal with turbulence-driven zonal flows. Our more realistic simulations in which zonal flows are self-consistently included found that the global mode structure is destroyed by the random shearing action of the zonal flows. This results predominantly in the reduction of the radial correlation length and subsequently the turbulence level [11]. This finding that the shearing of zonal flows is the dominant saturation mechanism represents a new nonlinear paradigm that is fundamentally different from that of the Hasegawa-Mima system [12], which has been popular because of its simplicity as a nonlinear paradigm for understanding drift wave turbulence. This motivated us to carefully study ρ^* scaling with self-generated zonal flows using large-scale simulations with device-size scans.

2 Size Scaling of Turbulent Transport

This study employs a well benchmarked, massively parallel full torus gyrokinetic toroidal code (GTC) [11] and uses representative parameters of DIII-D tokamak H-mode core plasmas which have a peak ion temperature gradient at $r = 0.5a$ with the following local parameters: $R_0/L_T = 6.9$, $R_0/L_n = 2.2$, $q = 1.4$, $\hat{s} \equiv (r/q)(dq/dr) = 0.78$, $T_e/T_i = 1$, $\epsilon \equiv r/R_0 = 0.18$. Here R_0 is the major radius, r is the minor radius, L_T and L_n are the temperature and density gradient scale lengths, respectively, T_i and T_e are the ion and electron temperatures, and q is the safety factor. These parameters [13] give rise to a strong ITG instability with a linear threshold of $(R_0/L_T)^{\rm crit} = 4.0$. These global simulations used fixed boundary conditions with electrostatic potential $\delta\phi = 0$ enforced at $r < 0.1a$ and $r > 0.9a$. The size of the tokamak is varied up to $a = 1000\rho_i$ with ρ_i measured at $r = 0.5a$ and other key dimensionless parameters fixed. The simplified physics model includes: a parabolic q profile, a pressure gradient profile of $\exp\{-[(r-0.5a)/0.3a]^6\}$, a circular cross section, no impurities, and electrostatic fluctuations with an adiabatic electron response. Externally driven plasma flows and collisions [14] are not treated in these simulations. In the full torus nonlinear simulation of $a = 1000\rho_i$, we calculated 7000 orbital time steps of one billion particles (guiding centers), and interactions of these particles with self-consistent electrostatic potential represented on 125 million spatial grid points to address realistic reactor-grade plasma parameters covering disparate spatial and temporal scales. These large scale simulations only became feasible recently with the implementation of an efficient global field-aligned mesh using magnetic coordinates, which reduces computational requirements by two orders of magnitude, and with the access to a multi-teraflop massively parallel computer, the fastest civilian computer in the world at the time of this study [15].

Each of these simulations starts with very small random fluctuations which grow exponentially due to the ITG instability. Zonal flows are then generated through the modulational instability [16, 17] and saturate the toroidal ITG eigenmodes through random shearing [18]. Finally, the nonlinear coupling of ITG-zonal flows leads to fully developed turbulence with a steady state transport level that is insensitive to initial conditions. The fluctuations in the steady state are nearly isotropic in the radial and poloidal directions. In contrast, when zonal flows are suppressed in the simulation, the radial spectra are narrower (dominated by low k_r components) for larger device sizes [19].

First, we quantify the fluctuation scale length. Radial correlation functions for the fieldline-averaged fluctuation quantities (density perturbations, etc.) are calculated using $r = 0.5a$ as a reference position, and averaged in the toroidal direction because of axisymmetry and over a few eddy turnover times, assuming statistically steady state. The correlation functions for density perturbations (or electrostatic potential excluding the zonal flow component) are found to be self-similar for different tokamak sizes (Fig. 1), and suggest a turbulent eddy size of $\sim 7\rho_i$ which is independent of device size. The correlation functions for temperature perturbations are very similar to those of the density perturbations, and the correlation functions for heat flux show a correlation length about half of those for density and temperature perturbations. All these correlation functions decay exponentially and no significant tails at large radial separations exist. We conclude that

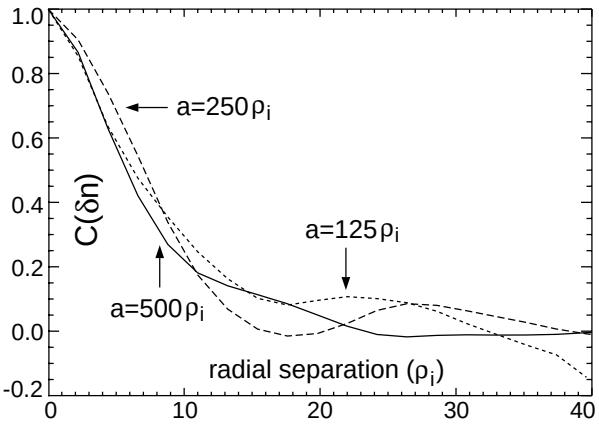

Figure 1: Radial correlation functions for density perturbations.

the fluctuation scale length is microscopic, i.e., on the order of ion gyroradius and independent of device size.

Next we examine whether transport is diffusive using the probability distribution function for the radial diffusion of test particles (passive particles that do not affect the turbulence). After nonlinear saturation, 6 million test particles are initiated around $r = 0.5a$ with a uniform poloidal distribution. The probability distribution function of radial displacement after a few eddy turnover times is found to be very close to a Gaussian. Further examination of the deviation from the Gaussian reveals no singular structure in either pitch angle or energy space. This indicates that there is no sharp resonance in the wave-particle interactions. Since the radial motion of test particles is diffusive rather than ballistic, the wave does not trap or convect the particles, but only scatters the particle orbits. We can calculate ion heat conductivity based on the random walk model of test particle heat flux, Q, due to the energy-dependent diffusivity $D = \sigma^2/2\tau$, $Q = -\int \frac{1}{2} v^2 D \partial f/\partial r d^3v$, where σ is the standard deviation for radial displacement at time τ after the initiation of test particles. We also measure the self-consistent heat flux, $Q = \int \frac{1}{2} v^2 \delta v_{E\times B} \delta f d^3v$, where v is particle velocity, δf is the perturbed distribution function, and $\delta v_{E\times B}$ is the radial component of gyrophase-averaged $E \times B$ drift. We found that the test particle heat flux is very close to the self-consistent heat flux. This suggests that wave transport, where the wave extracts energy from ions in the hot region and deposits it back to ions in the cold region, does not play a significant role. Furthermore, the probability distribution functions for the electrostatic potential, temperature fluctuations, and heat fluxes all decay exponentially with no significant tails at large amplitudes. This is observed for large devices where the transport scaling is gyroBohm, and where there are a large number of data samplings for adequate statistics. We conclude that the heat flux is carried by the radial diffusion of particles, and that large transport events, where heat pulses propagate ballistically, are apparently absent over this simulation time.

Now that the fluctuation scale length is found to be microscopic and test particle transport to be diffusive, we might expect the transport scaling to be gyroBohm. Surprisingly, local ion heat conductivity (Fig. 2) measured at $r = 0.5a$ in this scan exhibits Bohm-like scaling for plasmas corresponding to present-day tokamak experiments ($a < 400\rho_i$), even though the turbulence eddy size is independent of device size. This result is consistent with recent dimensionless scaling studies on the DIII-D tokamak, which found that ion transport and energy confinement time exhibit Bohm-like behavior while fluctuation characteristics suggest a gyro-Bohm scaling [7]. As we increase the device size further (up to $a = 1000\rho_i$), there is a gradual transition from Bohm-like scaling to gyroBohm scaling. Interestingly, recent transport studies of the JET tokamak [8] and a scan of power thresholds for the formation of internal transport barriers [20] show a similar trend. These findings show that extrapolations from present-day experiments to larger devices based on empirical scalings or mixing length rules can be unreliable.

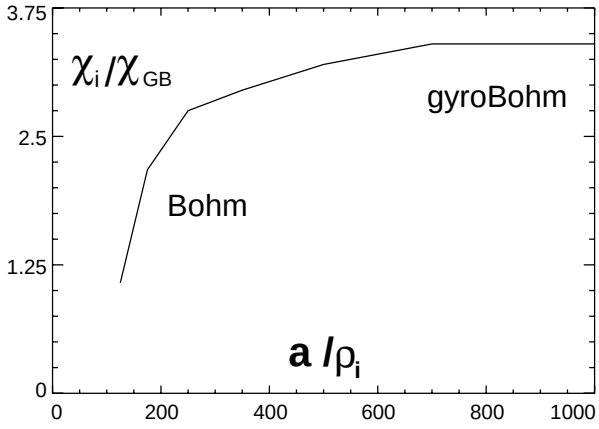

Figure 2: Ion heat conductivity vs. minor radius.

Possible mechanisms for the transition from Bohm scaling to gyroBohm scaling need to be identified. The device size where the transition occurs in the present studies is much larger than that expected from the linear ITG theory of pressure gradient profile variations. It is well known that strong profile variations in a small device can reduce the linear growth rate of the

ITG mode [3]. However, the results shown in Fig. 3 indicate that this effect is only important for $a < 100\rho_i$. The linear growth rates are found to become independent of device size when $a > 100\rho_i$ for both the most unstable linear mode ($k_\theta \rho_i \sim 0.45$) and the dominant nonlinear mode ($k_\theta \rho_i \sim 0.22$). Therefore, the transition from Bohm to gyroBohm should be governed by nonlinear processes.

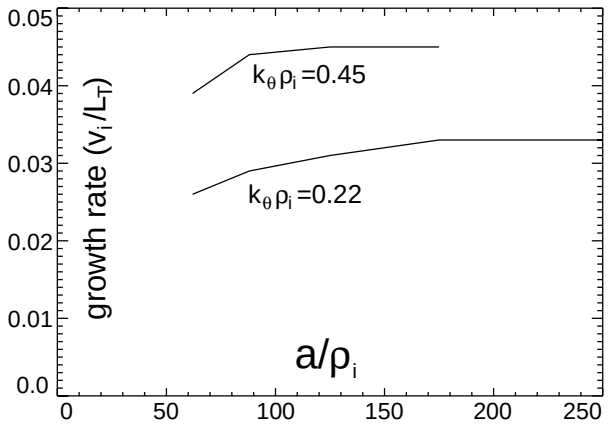

Figure 3: Linear growth rate vs. device size.

Previous two-dimensional fluid simulations of toroidal ITG modes have found that Bohm-like transport can be driven when the diamagnetic flow shear is a significant fraction of the linear growth rate near the ITG threshold [21], and that the scaling is always gyroBohm far away from marginality. However, zonal flows are not properly treated in that study. In the present simulations with zonal flows included, we have scanned the pressure gradient down toward the linear threshold, and found that turbulence is completely suppressed by zonal flows [13] before the shear of diamagnetic rotation becomes a significant fraction of the linear growth rate. In the simulation results shown in Fig. 2, the plasma is far away from linear marginality. In fact, the linear growth rates γ are comparable to mode real frequencies ω_r ($\gamma \sim \omega_r/2$ for $k_\theta \rho_i = 0.45$, and $\gamma \sim \omega_r/3$ for $k_\theta \rho_i = 0.22$). Profile relaxation has been observed in full torus simulations [22], which can drive the system toward marginality. To prevent this unrealistic relaxation, we use an effective collision operator for energy diffusion to model a heat bath: $\delta f_c = f_0[(v/v_{\mathrm{T_i}})^2 - 3/2]\delta T/T_i$, where δT is ion temperature perturbation averaged over the flux-surface and over a minor radius range of a few eddy sizes. The effective collision time of this operator is on the order of an ion energy confinement time, which is much longer than the turbulence decorrelation time. Ion temperatures are restored to their initial value using this heat source/sink. Thus pressure profiles are kept fixed throughout the simulations. Therefore, the Bohm-like scaling for small device size produced in our simulations is not due to marginality or profile relaxation.

It is found that the fluctuation amplitude (excluding zonal flows) scales as $\delta v_{E\times B} \propto v_{\mathrm{dia}}/\sqrt{\rho^*}$ in the Bohm regime for small devices, and $\delta v_{E\times B} \propto v_{\mathrm{dia}}$ in the gyroBohm regime for larger devices, where $v_{\mathrm{dia}} = v_i \rho_i / R_0$. This $\delta v_{E\times B}$ scaling, together with the fact that test particle transport is diffusive, indicates that the effect of sharp profile variations of the pressure gradient in a relatively small size plasma reduces the fluctuation amplitude through nonlinear processes and leads to Bohm-like transport. A plausible mechanism for this effect is the radial penetration of fluctuations from the unstable region to the linearly stable region [22, 21]. Indeed, it is observed that in the nonlinearly saturated phase, fluctuations spread radially toward both directions (edge and axis) for a region on the order of $25\rho_i$ independent of the device size. If we assume that total fluctuation energy content is not affected by this radial expansion, then the fluctuation intensity scales as $(\delta\phi)^2 \simeq \delta\phi_{\mathrm{GB}}/(1 + 50\rho_*)^2$, where $\delta\phi_{\mathrm{GB}} \simeq \rho^* T_e/e$ is the gyroBohm scaling for $\rho^* \to 0$. Since $\chi_i \propto |\delta\phi|^2$ has previously been observed [14], the heat conductivity should then scale as $\chi_i \simeq \chi_{\mathrm{GB}}/(1 + 50\rho_*)^2$. Interestingly, this heuristic scaling formula fits well the simulation results.

3 Turbulence Spreading and Transport Scaling

Our recent global gyrokinetic simulations[23] of ITG turbulence described in the previous section show that the turbulence intensity propagates in space, to regions where the ITG modes are linearly stable. This constitutes a type of non-local transport phenomenon. Here, we present a simple one dimensional nonlinear model of turbulence propagation[24] which is similar to previous models of transport barrier propagation[25] and ground water spreading in porous rock[26].

$$\frac{\partial}{\partial t}I = \gamma(x)I - \alpha I^2 + \chi_0 \frac{\partial}{\partial x}(I\frac{\partial}{\partial x}I). \tag{1}$$

Here I is the dimensionless turbulence intensity, x is a radial coordinate, and $\gamma(x)$ is the "local" growth rate of the ITG mode which depends on the local gradient in ion temperature. We take $\gamma(x)$ to be monotonically decreasing in x, i.e., $\gamma(x) > 0$ for $x < x_0$ and $\gamma(x) < 0$ for $x > x_0$. The α term represents a local nonlinear coupling which is responsible for a local nonlinear saturation of turbulence. $\chi_0 I$ is a turbulent diffusivity with an explicit proportionality to I as observed in the previous gyrokinetic simulation[14]. In the absence of the last term, Eq. (1) yields a nonlinear saturation level $I(x) = \gamma(x)/\alpha$ which is non-zero only in the region $\gamma(x) > 0$. Now we study the role of the last term, describing the radial diffusion of turbulence in fluctuation propagation. Since we are primarily interested in the region where $\gamma(x) \simeq 0$ and I is consequently small, it is instructive to look at the behavior of a solution of the following nonlinear equation,

$$\frac{\partial}{\partial t}I_0 = \chi_0 \frac{\partial}{\partial x}(I_0\frac{\partial}{\partial x}I_0) \tag{2}$$

With an initial profile

$$I_0(x,0) = \frac{4Q}{x_0}(1 - \frac{x^2}{x_0^2})H(x_0 - x),$$

which can be matched to a local saturation level $\gamma(x)/\alpha$ for an appropriate choice of parameters, Eq. (2) has the following exact solution:

$$I_0(x,t) = \frac{4Q}{(24Q\chi_0 t + x_0^3)^{1/3}}(1 - \frac{x^2}{(24Q\chi_0 t + x_0^3)^{2/3}})H((24Q\chi_0 t + x_0^3)^{1/3} - x), \tag{3}$$

where H is an Heaviside function.

In the absence of linear or nonlinear damping (the first and second terms on the RHS of Eq. (1)), the front at $x = (24Q\chi_0 t + x_0^3)^{1/3}$ will propagate beyond x_0 indefinitely. We expect that this front propagation would be stopped or significantly reduced when the increase of I for $x > x_0$ due to nonlinear diffusion is balanced by an ever-increasing linear damping of I as x increases. By taking

$$\frac{\partial}{\partial t}\int_{x_0}^{x_0+\Delta} dx I(x,T) = -\int_{x_0}^{x_0+\Delta} dx \gamma(x,T) I_0(x,T),$$

we obtain a relation between the front location at saturation and the time T for the front saturation to take place. For $x_0 >> \Delta, (24Q\chi_0 T)^{1/3}$, we get $\Delta^2 \simeq 16\chi_0/(\gamma' x_0^2)$, where $\gamma(x_0 + \Delta) \simeq \gamma'\Delta$ has been used. Using the values of χ_0, γ' and $x_0 \simeq 3/8$ from our nonlinear ITG simulation, we obtain $\Delta \simeq 14\rho_i$ which is in the rough range of fluctuation broadening observed in our simulation, $\Delta \simeq 25\rho_i$.

4 Global vs. Local Comparisons

Our global simulations in Section 2 used a toroidal geometry including finite aspect ratio effects [23], while local simulations in the Cyclone benchmark [13] ignored finite aspect ratio effects. In this Section, we simplify our geometry to remove finite aspect ratio effects in order to compare with the local simulations. We found that the linear growth rate for the most unstable mode in our global GTC simulations with $a = 250\rho_i$ is identical (Fig. 4) to that obtained in a Cyclone flux-tube simulation of Dimits *et al* [13]. Similar agreement was also obtained for comparisons of linear mode frequencies.

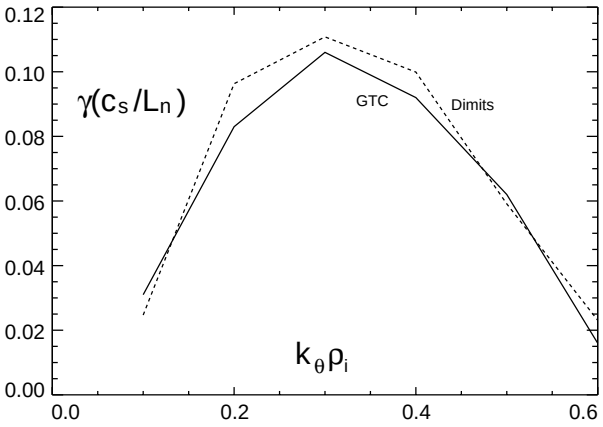

Figure 4: Linear growth-rate comparisons.

We scanned the device size up to the Gyro-Bohm regime in our nonlinear global simulations and compared the ion heat conductivities to the results of flux-tube simulations, Fig 5. The global simulation results for large device size is shown to be close to those of local simulations [13]. Note that there are some differences between global and local simulations in term of geometry. Local parameters such as q, s, ϵ are constant in local simulations, but are functions of minor radius in global simulations. The radial box size in the local simulation is $128\rho_i$, which is much smaller than that in global simulations. Local simulations use periodic boundary condition in the radial direction, while global simulations use a fixed radial boundary condition. Considering these differences in equilibrium geometry, the agreement between global and local nonlinear simulations appears to be acceptable.

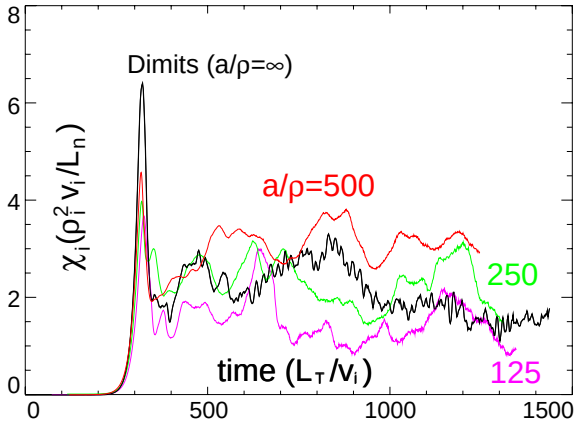

Figure 5: Time history of ion heat conductivity.

Using an energy source/sink as discussed in Section 2, we can extend the simulation time to hundreds of turbulence decorrelation times. Quasi-steady state ion heat conductivity, turbulence fluctuation energy, and zonal flow energy are plotted in Fig. 5 and Fig. 6, respectively. Such long simulation times provide reliable statistics for temporal correlation analysis. However, it should be pointed out that the energy source/sink, as any model used in the turbulence simulation community, is not from first-principles. Quantitative differences result from using various models, although the qualitative trend is preserved. No numerical instability is observed during the long simulation time.

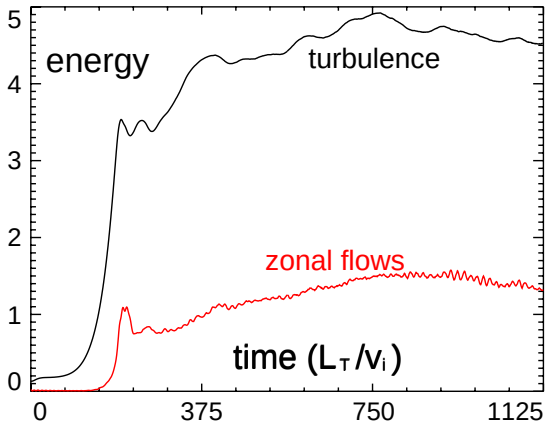

Figure 6: Time history of turbulence energy and zonal flow energy for $a = 500\rho_i$.

5 Role of Trapped Electron Nonlinearity in Zonal Flow Growth in TEM Turbulence

While significant progress has been made in understanding the interaction of zonal flows and ITG turbulence, there has been little advance in understanding the zonal flow behavior in trapped electron mode (TEM) turbulence. For pure ITG turbulence where the electron response is adiabatic, the modulation of ion polarization density leads to zonal flow growth[16, 17]. While it has been stated that the expected trapped electron nonlinearity for TEM turbulence would be subdominant to the ion nonlinearity by an order of $\sqrt{\epsilon}$ in the context of the Wave Kinetic approach, a cancellation between the radial modulation in trapped electron density and the modulation in ion gyrocenter density has been proposed as a possible reason for dominance of streamers (with relatively weak zonal flows) in TEM turbulence from a preliminary flux-tube gyrokinetic simulation[27].

Here, we estimate the role of the trapped electron nonlinearity in zonal flow generation quantitatively in the context of a four wave parametric instability theory in toroidal geometry[17]. We follow the usual weak turbulence expansion for fluctuations with a single non-zero toroidal mode number n involving the pump TEM ϕ_0, the side band TEM's ϕ_+ and ϕ_-, and the zonal flow mode ϕ_Z. The Hasegawa-Mima type nonlinear coupling of ϕ_0 and $\phi_{+,-}$ is balanced by the neoclassically enhanced polarization shielding of the zonal flow potential ϕ_Z as described in Eq. (3) of the Ref.[17]. Because the trapped electron banana width is much smaller than the trapped ion banana width, and $\nu_{ee}\rho_e/(\nu_{ii}\rho_i) \simeq \sqrt{(m_e/M_i)}$, the shielding of ϕ_Z on the left hand side of Eq. (3) is not changed; therefore the presence of trapped electrons can modify the balance of the nonlinear polarization current and the neoclassical polarization current only through modification of the linear susceptibility α_i of the pump TEM in that equation.

On the other hand, the nonlinear excitation of the linearly damped side bands $\phi_{+,-}$ through $\mathbf{E}\times\mathbf{B}$ nonlinear coupling between ϕ_0 and ϕ_Z is described by the quasi-neutrality condition for the density responses obtained from the nonlinear ion gyrokinetic equation (Eq. (4) of Ref. [17]) and the trapped electron nonlinear bounce kinetic equation. We find that the trapped electrons merely reduce the $\mathbf{E}\times\mathbf{B}$ nonlinearity (which has no explicit mass dependence), which produces side band fluctuations via the zonal flow modulation, by a factor of $\sqrt{8\epsilon}/\pi$, i.e., the surface averaged fraction of trapped electron population (The right hand side of Eq. (4) in Ref.[17] should be multiplied by $(1-\sqrt{8\epsilon}/\pi)$.

Therefore we conclude that:

1. a partial cancellation between the radial modulation in trapped electron density and the modulation in ion gyrocenter density is not likely to reduce the zonal flow growth rate in TEM turbulence significantly, and

2. most of the zonal flow growth rate change due to trapped electrons may occur via changes in linear properties such as the side band damping rate and the linear susceptibility (dispersion relation) of the pump TEM.

This work is supported by US DOE Contract No. DE-AC02-76CH03073 (PPPL), grand number DE-FG03-94ER54271 (UC Irvine), Grant number 88ER53275 (UCSD), and in part by the DOE SciDAC plasma microturbulence project.

References

[1] M. Wakatani, *et al.*, *Nuclear Fusion* **39**, 2175 (1999).

[2] J. W. Connor and J. B. Taylor, *Nuclear Fusion* **17**, 1047 (1979).

[3] W. Horton, *Rev. Modern Physics* **71**, 735 (1999).

[4] A. M. Dimits, *et al.*, *Phys. Rev. Lett.* **77**, 71 (1996).

[5] F. W. Perkins, *et al.*, *Phys. Fluids B* **5**, 477 (1993).

[6] C. C. Petty, *et al.*, *Phys. Plasmas* **9**, 128 (2002).

[7] G. McKee, *et al.*, *Nuclear Fusion* **41**, 1235 (2001).

[8] R. V. Budny, *et al.*, *Phys. Plasmas* **7**, 5038 (2000).

[9] W. W. Lee, *Phys. Fluids* **26**, 556 (1983).

[10] Y. Kishimoto, *et al.*, *Phys. Plasmas* **3**, 1289 (1996), and references therein.

[11] Z. Lin, *et al.*, *Science* **281**, 1835 (1998).

[12] A. Hasegawa and K. Mima, *Phys. Fluids* **21**, 87 (1978).

[13] A. M. Dimits, *et al.*, *Phys. Plasmas* **7**, 969 (2000).

[14] Z. Lin, *et al.*, *Phys. Rev. Lett.* **83**, 3645 (1999).

[15] W. M. Tang, *Phys. Plasmas* **9**, 1856 (2002).

[16] P. H. Diamond, et al., in Proceedings of the 17th IAEA Conference on Controlled Fusion and Plasma Physics, Yokahama, Japan, 1998.

[17] Liu Chen, *et al.*, *Phys. Plasmas* **7**, 3129 (2000).

[18] T. S. Hahm, *et al.*, *Phys. Plasmas* **6**, 922 (1999).

[19] T. S. Hahm, *et al.*, *Plasmas Phys. Contr. Fusion* **42**, A205 (2000).

[20] G. T. Hoang, "Additional Heating Power required for ITB formation in Tokamaks", in proceeding of 28th European Physical Society Conference on controlled Fusion and Plasma Physics, Montreux, Switzerland, 2002.

[21] X. Garbet and R. E. Waltz, *Phys. Plasmas* **3**, 1898 (1996).

[22] S. E. Parker, *et al.*, *Phys. Rev. Lett.* **71**, 2042 (1993).

[23] Z. Lin, *et al.*, Phys. Rev. Lett. **88**, 195004 (2002).

[24] T. S. Hahm, P.H. Diamond, and Z. Lin, "Turbulence Spreading and Tokamak Transport Scaling" *Presented at ITPA Transport/ITB Physics Topical Group Third Meeting, Cadarache, France, October 2002*.

[25] P. H. Diamond, *et al.*, Phys. Rev. Lett. **78**, 1472 (1997).

[26] G. I. Barenblatt, *Dimensional Analysis* (Gordon and Breach, New York, 1987).

[27] W. M. Nevins, 2nd US/Korea Bilateral Transport Workshop, August (2002).